Desalination and Water Treatment
www.deswater.com

36 (2011) 34–40
December

1944-3994/1944-3986
doi: 10.5004/dwt.2011.1427

Impact of anionic surfactants on oxygen transfer rate in the electroflotation process

M. Kotti, I. Ksentini, L. Ben Mansour*

Unité de recherché, Mécanique des fluides appliquée et modélisation, Faculté des sciences de Sfax, B.P.1171, 3000 Sfax, Tunisie
Tel.: +21698657061; Fax: +21674666479; email: lassaadbenmansour@yahoo.fr

Received 12 December 2009; accepted 10 April 2011

ABSTRACT

This work concerns the treatment of liquid effluents rich in anionic surfactant by the electroflotation process in batch mode. The oxygen transfer was studied considering its importance for the abatement of the dissolved organic matter in the industrial effluents. The volumetric mass transfer coefficient (K_La) which is the key parameter in the characterisation of transfer process was evaluated for different values of current density and various surfactant concentrations. The volumetric mass transfer coefficient was also dissociated to evaluate the liquid-side mass transfer coefficient (K_L) and specific interfacial area (a). The K_L decreases with the anionic surfactant concentration until the critical micelle concentration and then it has undergone a notable increase, the specific interfacial area decreases with the anionic surfactant. Models of (K_L) have been established to describe the effects of the operational parameters as well as the physicochemical characteristics of the liquid phase on the oxygen transfer.

Keywords: Electroflotation; Mass transfer coefficient; Current density; Anionic surfactant

1. Introduction

Anionic surfactants are extensively used in many fields of technology and research due to their favourable physicochemical characteristics [1]. These surfactants enhance the solubility of sparingly soluble compounds in water and can affect the mass transfer from the gas to the liquid phase [2–7]. However, wastewater rich on anionic surfactants issued from different industrial processes such as lubrication, metallurgy, petrol and textile finishing industry raises a series of environmental problems [8]. The electrochemical techniques have an important role to treat this wastewater emission.

Electroflotation (EF) is an electrochemical process that floats pollutants to the surface of water by tiny bubbles of hydrogen and oxygen generated from electrolysis of aqueous solutions [9–14]. The electrochemical reactions at the cathode and anode are, therefore, mainly hydrogen and oxygen evolution, respectively.

$$\text{Anodicoxidation}: 2H_2O \rightarrow O_2^- + 4H^+ + 4e^- \quad (1)$$

$$\text{Cathodicreduction}: 4H_2O + 4e^- \rightarrow 2H_2^{\uparrow} + 4OH^- \quad (2)$$

The effectiveness of the process is limited not only to the elimination of the polluting substances but also to the abatement of the dissolved organic matter by oxygen generated at the anode. Most available EF process data has shown the effect of EF process in decreasing

*Corresponding author

chemical oxygen demand (COD) but without detailing the transfer phenomena [15–18].

The objective of the present study is to investigate the effect of anionic surfactant solutions on oxygen transfer rate and to evaluate separately the liquid-side mass transfer coefficient K_L and the interfacial area (a).

2. Theory

In the absence of chemical reaction, gas–liquid mass transfer to a low solubility gas bubble is controlled by molecular diffusion in the liquid phase [19]. Lewis and Whitman assumed that the gas side resistance is negligible and that the gas transfer may be determined from considering the liquid side resistance only [20]:

$$\frac{dC}{dt} = K_L a(C^* - C), \tag{3}$$

where dC/dt is the rate of change of oxygen concentration with time.

Eq. (3) can be readily integrated to yield the following expression for C as a function of time:

$$C = C^* - (C^* - C_0)\ \exp(-K_L a\, t), \tag{4}$$

where C_0 is the initial dissolved oxygen concentration at $t = 0$. A nonlinear regression analysis based on the Gauss–Newton method is recommended by ASCE (American Society of Civil Engineers) to fit Eq. (4) to experimental data using $K_L a$, C^* and C_0 as three adjustable model parameters [21].

The volumetric mass transfer coefficient must be corrected to a standard reference temperature of 20°C by using the Arrhenius relationship [19]:

$$K_L a_{(20°C)} = K_L a_{(T)} \theta^{(20-T)}. \tag{5}$$

A generally accepted value of the temperature correction factor, θ is 1.024 [22].

3. Experimental set-up and measuring techniques

3.1. EF cell

The EF cell, shown in Fig. 1, is used for batch mode. It is a cylindrical plexiglas vessel and is 9.20 cm in diameter and 71.5 cm in height. It is provided with two electrodes: titanium coated with ruthenium oxide anode and a stainless steel cathode. These two electrodes are supplied by a generator of DC current which enables the variation of current density. It is also noticed that the gap between anode and cathode was maintained at 5 mm to minimize the ohmic loss. The cathode compared to perforated anode occupies the top position. This perforation allows the evacuation of bubbles produced at the anode [23].

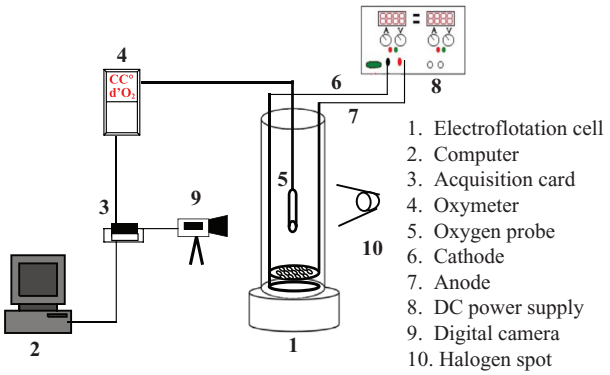

Fig. 1. Experimental set-up.

3.2. Image analysis

The equipments used for the determination of the bubble size distributions by image analysis were a microscopic zoom digital video camera (model NV-A3E from Panasonic, Japan), an acquisition card (model Pinnacle PCTV PRO version 4.02 from Pinnacle systems), a PC (model Pentium 4, from Fujitsu Siemens) with a digital image analysis programs namely: Photofiltre (Version 6.2.6), Photoshop (CS2), Ulead Photo Impact (Version 11 Pro) and 700 W power halogen spot.

A wire of known diameter was video taped for use as the calibration factor for the bubble size. For getting a sufficient representative bubble size distribution usually sizes of at least 100 bubbles were determined.

3.2.1. Gas hold-up

Gas hold-up is a dimensionless key parameter defined as the volume fraction of gas phase occupied by the gas bubbles [24].

The gas hold-up is calculable in the following way using image treatment system [19]:

$$\varepsilon_g = \frac{\Delta H}{\Delta H + H_L}, \tag{6}$$

where ΔH is the increase in liquid level after gassing.

3.2.2. Volumetric mass transfer coefficient

The volumetric mass transfer coefficient $K_L a$ was measured using the unsteady state method with an oxygen probe (Consort C932) placed mid-way in the EF cell. The oxygen concentration was reduced to zero by adding 150 mg/L of sodium sulphite (Na_2SO_3) and 2 mg/L of cobalt ions [25].

Table 1
Chemical characteristics of liquid phases in the ambient conditions

Solution type	Surfactant	CMC [g/L]	C_{ST} [g/L]	Liquid density [kg/m^3]	Liquid surface tension [N/m]	Liquid viscosity [Pa.s]
Clean tap water	–	–	–	1,000	0.07275	0.001
Anionic surfactant	Sodium polymethacrylate	0.25	0.1	997,455	0.06748	0.00125
			0.25	995,866	0.05747	0.00182
			0.5	993,144	0.05548	0.00283
			1	985,176	0.05447	0.00579
			1.5	983,488	0,05315	0,00874

$$2\,Na_2SO_3 + O_2 \rightarrow 2\,Na_2SO_4 \quad (7)$$

Experiments were conducted with different model anionic surfactant solutions (Table 1) at current density ranging from 60 to 260 A/m^2.

3.2.3. The specific interfacial area

The specific interfacial area is one of the most important parameters for gas-liquid reactor design. Once the gas hold-up and bubble diameter are measured the specific interfacial area (a) could determined using the following equation [26]:

$$a = \frac{6\,\varepsilon_g}{d_B(1-\varepsilon_g)}. \quad (8)$$

3.2.4. The liquid-side mass transfer coefficient K_L

Measurement of mass transfer coefficient K_La and the specific interfacial area (a) allows the determination of the liquid-side mass transfer coefficient K_L:

$$K_L = \frac{K_La}{a}. \quad (9)$$

3.3. Liquid-phase characterization

Table 1 presents the variety of liquid phase characteristics which allows understanding the effect of surfactant solutions on the mass transfer efficiency.

It is well known that surfactants are characterized by critical micelle concentrations (CMC). The CMC is the concentration where surfactant molecules arrange themselves into organized molecular assemblies known as micelles [27].

The CMC of anionic surfactant in water is determined from measurements of the specific conductivity vs. the surfactant concentration by Consort C932 at 20°C [28].

4. Results and discussion

In order to calculate the volumetric mass-transfer coefficients from the ASCE model using Eq. (4) a series of unsteady states reoxygenation tests at different current densities and concentrations of anionic surfactant were conducted.

All the data are exploited by a specific data-processing program which is (DataFit version 8.1.69). The principle of this method is to make a non-linear regression of the exponential form of the transfer equation.

Fig. 2 shows a fast evolution of the oxygen concentration, then stabilization due to the saturation of the liquid solution with dissolved oxygen time.

4.1. Effect of anionic surfactant on K_La

The volumetric mass transfer coefficient K_La is plotted as a function of the anionic surfactant concentration at different current densities.

As shown in Fig. 3 the volumetric mass transfer coefficient K_La decreases with the anionic surfactant concentration until the CMC (0.25 g/L), in this case a

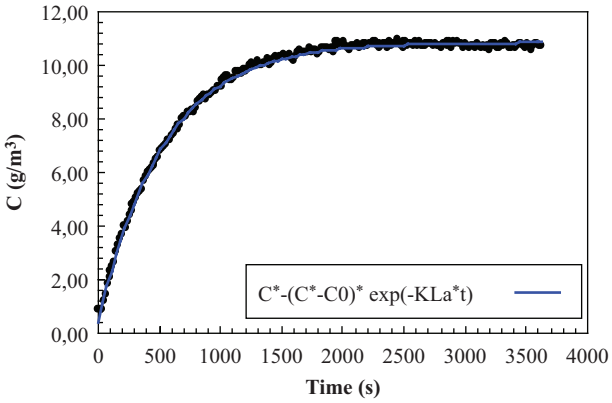

Fig. 2. Example of non-linear regression of experimental data by DataFit for clean tap water at 100 A/m^2.

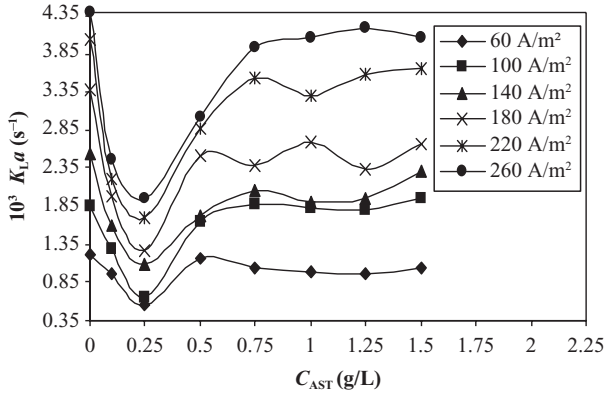

Fig. 3. Variation of the volumetric mass transfer coefficient as a function of anionic surfactant concentration.

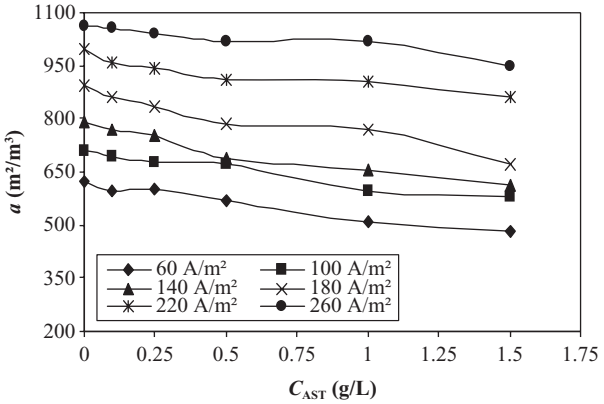

Fig. 5. Variation of specific interfacial area as a function of anionic surfactant concentration.

uniform layer of surfactant is adsorbed at the interface gas-liquid (screen effect for the passage of the bubble gas to the interface) which offers an additional resistance to the oxygen transfer and consequently reduction in K_La.

From the CMC K_La has undergone a notable increase: the molecules of surfactant arrange themselves into micelles which minimize the initial surface molecular solvated state in water; this last phenomenon decreases the screen effect, thus reduces the resistance of exchange and consequently improves the oxygen transfer.

The K_La stabilizes for the large concentrations higher than (0.75 g/L). This stabilization can be explained by limiting transfer.

Fig. 4 shows that, whatever the liquid phases, the volumetric mass transfer coefficient K_La increases with the current density. It is also noted that the volumetric mass transfer coefficients K_La of anionic surfactant solution are significantly smaller than those of water.

4.2. Effect of anionic surfactant on specific interfacial area

The variations of specific interfacial area with the anionic surfactant concentration are plotted in Fig. 5 for different current densities.

Fig. 5 shows that whatever the current densities, the specific interfacial area decrease with the anionic surfactant concentration.

The anionic surfactant has a double effect: on the one hand it supports coalescence by its viscosity and on the other hand it decreases the surface tension [Table 1]. These two effects are opposed: the coalescence increases the bubble diameter, but on the other side the decease of the surface tension reduces the bubble size [29].

According to Fig. 5 we can deduce that the coalescence effect carry on the surface tension effect to support the increase in the bubble diameter and as a result reduction in the specific interfacial area.

As shown in Fig. 6 whatever the liquid phases, the specific interfacial area increases with the current

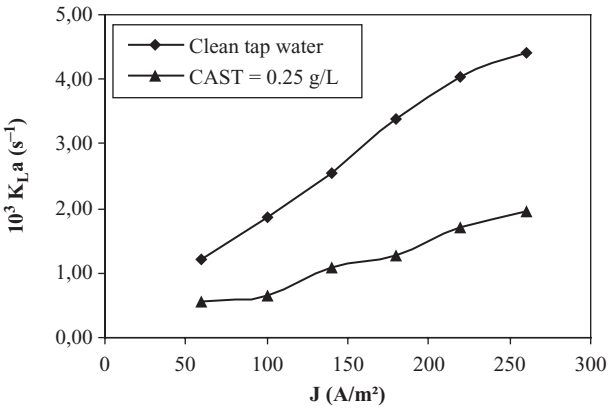

Fig. 4. Variation of the volumetric mass transfer coefficient as a function of current density.

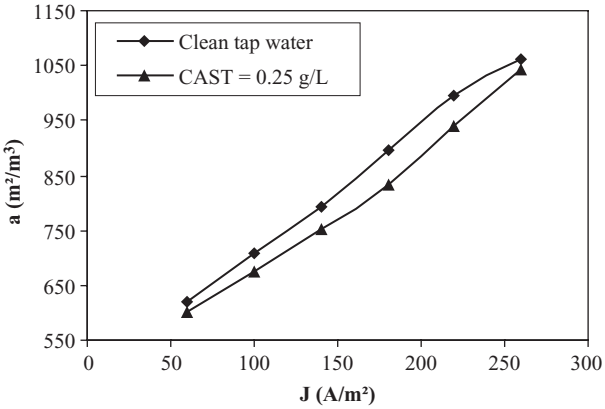

Fig. 6. Variation of the interfacial area as a function of current density.

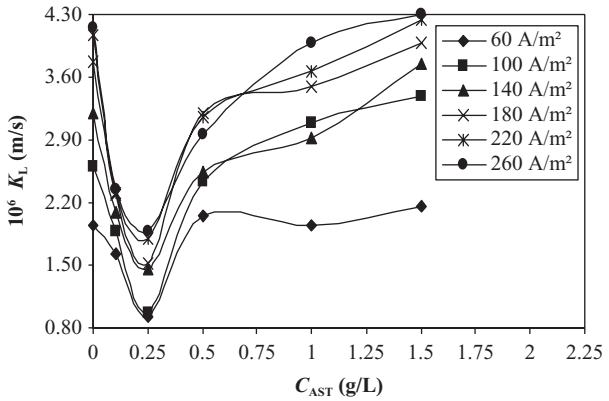

Fig. 7. Variation of the liquid-side mass transfer coefficient as a function of anionic surfactant concentration.

density. In fact, when the current density increases, the number of oxygen bubbles increases, too. This suggests an amelioration in the exchange surface.

4.3. *Effect of anionic surfactant on* K_L

The liquid-side mass transfer coefficient is plotted as a function of the anionic surfactant concentration at different current densities.

As shown in Fig. 7 the liquid-side mass transfer coefficient K_L decreases with the anionic surfactant concentration until the CMC (0.25 g/L), from which K_L has undergone a notable increase.

According to Fig.7, the variation of liquid-side mass transfer coefficient K_L with the concentration of anion surfactant are similar to that of $K_L a$ for different current densities (Fig. 3), this confirms that liquid-side mass transfer coefficient K_L carry on the specific interfacial surface (a) during the process of transfer.

As showing in Fig. 8, whatever the liquid phase, the K_L value increases with increasing current density,

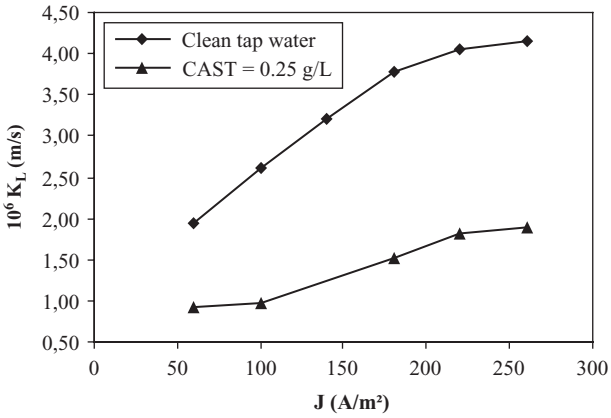

Fig. 8. Variation of the liquid-side mass transfer coefficient as a function of current density.

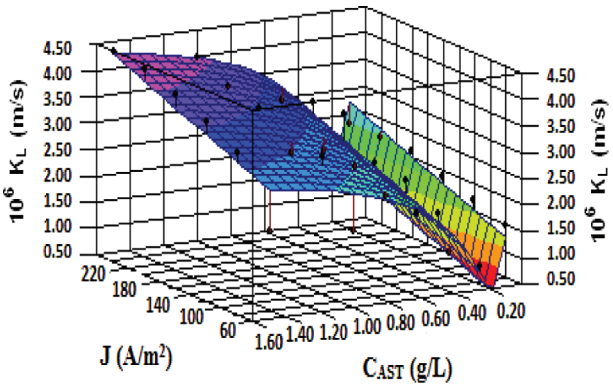

Fig. 9. Experimental values of K_L in comparison with the values considered by the model.

when J reached higher values than 220 A/m^2, (K_L) trend to stabilize.

When the current density increases, the number of oxygen bubbles increases, too. The increase of the number of bubbles generates an intense agitation which decrease the transfer resistance in the liquid phase and increase the liquid-side mass transfer coefficient.

The liquid-side mass transfer coefficient K_L related to the anionic surfactant solutions are significantly smaller than those of water.

5. Modeling of data

In order to explain the results of the present studies the mathematical model that permits to express the liquid-side mass transfer coefficient according to operation conditions such as the current density and the anionic surfactant concentrations was selected. For this objective, an appropriate mathematical program DataFit (version 8.1.69) that permitted to find this model was used and the following model was obtained [23].

$$K_L = 3.19 \times 10^{-6} + 6.54 \times 10^{-9}.J - \frac{9.97 \times 10^{-7}}{C_{AST}} + \frac{7.82 \times 10^{-8}}{C_{AST}^2}. \quad (10)$$

The comparison between the experimental values of the liquid side-mass transfer coefficient and the values predicted by the model (Eq. (10)) is presented in Fig. 9. As shown in this figure the obtained model fits the experimental data very well.

6. Comparison with other aeration system

The results found with the present EF process are compared with that obtained by gas-distributor [30] (Table 2).

Table 2
Comparison between the results of oxygen transfer parameters obtained by the electroflotation process and gas-distributor

Type	Aeration systems	Interfacial aeria (a) (m^2/m^3)	Mass transfer coefficient	
			K_La (s^{-1})	K_L (m/s)
Clean tap water	Gas-distributor	3.1–11.2	3.67×10^{-4}–4.13×10^{-3}	1.02×10^{-4}–4.07×10^{4}
	Electroflotation	621.6—1061.7	1.21×10^{-3}–4.4×10^{-3}	1.94×10^{-6}–4.14×10^{-6}
Anionic surfactant	Gas-distributor	3.9-12	3.8×10^{-4}–2.13×10^{-3}	8.96×10^{-5}–1.64×10^{-4}
	Electroflotation	599.9–1042.4	5.60×10^{-4}–1.96×10^{-3}	9.33×10^{-7}–1.88×10^{-6}

It is noticed that the volumetric mass transfer coefficient K_La provided by the EF process for different liquid solutions is comparable to other aeration systems. Indeed, the EF process gives the highest specific interfacial area and a smaller liquid-side mass transfer coefficient K_L. A mechanical agitation was proposed in order to minimize the transfer resistance and improve K_L.

7. Conclusion

It appears that the concentration of surfactant affect significantly the interfacial area and the transfer phenomena gas-liquid. In fact, the results of analysis prove the presence of the screen effect which disadvantages oxygen transfer in the presence of anionic surfactant as well as the influence of the CMC on this phenomenon.

The dissociation of volumetric mass transfer coefficient K_La enabled us to deduce that:

- The specific interfacial area tends decreases with the anionic surfactant.
- The effects of anionic surfactant concentration on the volumetric mass transfer coefficient and the liquid-side mass transfer coefficient are similar.

The simple model for estimation of K_L based on the current density and anionic surfactant concentration are established.

Symbols

a	specific interfacial area (m^2/m^3)
C	dissolved oxygen concentration in liquid phase (kg/m^3)
C^*	equilibrium oxygen concentration in liquid phase (kg/m^3)
C_{AST}	anionic surfactant concentration (kg/m^3)
C_{ST}	surfactant concentration (kg/m^3)
CMC	critical micelle concentration (kg/m^3)
d_B	bubble diameter (m)
H_L	ungassed liquid height (m)
J	current density (A/m^2)
K_L	liquid-side mass transfer coefficient (m/s)
K_La	volumetric mass transfer coefficient (s^{-1})
T	temperature (°C)
t	time (s)

Greek symbols

θ	theta factor
ε_g	gas hold-up

Subscripts

g	gas
L	liquid
ST	surfactant
AST	anionic surfactant

References

[1] T. Cserhati, E. Forgacs and G. Oros, Biological activity and environmental impact of anionic surfactants, Env. Inter., 28 (2002) 337–348.
[2] W.W. Eckenfelder and E.L. Barnhart, The effect of organic substances on the transfer of oxygen from air bubbles in water, AIChE. J., 7 (1961) 631–634.
[3] K. Koide, S. Yamazoe and S. Harada, Effects of surface active substances on gas holdup and gas liquid mass transfer in bubble column, J. Chem. Eng. Jpn., 18 (1985) 287–292.
[4] J.J. Jeng, J.R. Maa and Y.M. Yang, Surface effects and mass transfer in bubble column, Ind. Eng. Chem. Process. Des. Dev., 25 (1986) 974–978.
[5] F. Kudrewizki and P. Rabe, Hydrodynamics and gas absorption in gassed stirred tanks in presence of tensides, Chem. Eng. Sci., 42 (1987) 1939–1944.
[6] F. Kawase and M. Moo-Young, The effect of antifoam agents on mass transfer in bioreactors, Bioprocess Eng., 5 (1990) 169–173.
[7] Morão, C.I. Maia, M.M.R. Fonseca, J.M.T. Vasconcelos and S.S. Alves, Effect of antifoam addition on gas–liquid mass transfer in stirred fermenters, Bioprocess Eng., 20 (1999) 165–172.
[8] S.H. Wu and P. Pendleton, Adsorption of anionic surfactant by activated carbon: Effect of surface chemistry, ionic strength, and hydrophobicity, J. Coll. Inter. Sci., 243 (2001) 306–315.
[9] V. Srinivasan and M. Subbaiyan, Electroflotation studies on Cu, Ni, Zn and Cd with ammonium dodecyl dithiocarbamat, Sep. Sci. Technol., 24 (1989) 145–150.
[10] A.Y. Hosny, Separating oil from oil–water emulsions by electroflotation technique, Sep. Technol., 6 (1996) 9–17.

[11] S.E. Burns, S. Yiacoumi and C. Tsouris, Microbubble generation for environmental and industrial separations, Sep. Purif. Technol., 11 (1997) 221–232.
[12] Y.K. Jung and M.Y. Han, Simultaneous removal of cadmium and turbidity in contaminated soil-washing water by electroflotation, Water Sci. Technol., 46 (11–12) (2002) 225–230.
[13] R.G. Casqueira, M.L. Torem and F.O. Cunha, Removal of heavy/ toxic metal by electroflotation, Saneamento Ambiental. São Paulo, 85 (2002) 46–51.
[14] G. Chen, Electrochemical technologies in wastewater treatment, Sep. Purif. Technol., 38 (2004) 11–41.
[15] N.M. Mostefa and M. Tir, Coupling flocculation with electroflotation for waste oil/water emulsion treatment optimisation of the operating conditions, Desalination, 161 (2004) 115–121.
[16] J. Ge, J. Qu, P. Lei and H. Liu, New bipolar electrocoagulation-electroflotation process for the treatment of laundry wastewater, Sep. Puif. Technol., 36 (2004) 33–39.
[17] M. Murugananthan, G.B. Raju and S. Prabhakar, Separation of pollutants from tannery effluents by electroflotation, Sep. Purif. Technol., 40 (2004) 69–75.
[18] L. Ben Mansour, Y. Ben Abdou and S. Gabsi, Effects of some parameters on removal process of nickel by electroflotation, Water Waste Environ. Res., 2 (2001) 51–58.
[19] J.M.T. Vasconcelos, J.M.L. Rodrigues, S.C.P. Orvalho, S.S. Alves, R.L. Mendes and A. Reis, Effect of contaminants on mass transfer coefficients in bubble column and airlift contactors, Chem. Eng. Sci., 58 (2003) 1431–1440.
[20] W.K. Lewis and W.G. Whitman, Principles of gas absorption, Ind. Eng. Chem., 16 (1924) 1215–1220.
[21] ASCE. Standard Measurement of Oxygen Transfer in Clean Water. American Society of Civil Engineers. 1984.
[22] J.M. Chern, S.R. Chou and C.S. Shang, Effects of impurities on oxygen transfer rates in diffused aeration systems, Water Res., 35 (2001) 3041–3048.
[23] M. Kotti, N. Dammak, I. Ksentini and L. Ben mansour, Effects of impurities on oxygen transfer rate in the electroflotation process, Ind. J. Chem. Technol. 16 (2009) 513–518.
[24] N. Kantarci, F. Borak and K.O. Ulgen, Bubble column reactors, Process Biochem., 40 (2005) 2263–2283.
[25] L. Ben Mansour, K. Kolsi and I. Ksentini, Influence of current density on oxygen transfer in an electroflotation cell, J. Appl. Electrochem., 37 (2007) 887–892.
[26] M. Bouaifi, G. Hebrard, D. Bastoul and M. Roustan, A comparative study of gas hold-up, bubble size, interfacial area and mass transfer coefficients in stirred gas–liquid reactors and bubble columns, Chem. Eng. Process. 40 (2001) 97–111.
[27] A. Dominguez, A. Fernandez, N. Gonzalez, E. Iglesias and L. Montenegro, Determination of critical micelle concentration of some surfactant by three techniques, J. Chem. Educ., 74 (1997) 1227–1231.
[28] T. Inoue, T. Misono and S. Lee, Comment on ''Determination of the critical micelle concentration of dodecylguanidine monoacetate (dodine)'', J. Colloid Interf. Sci., 314 (2007) 334–336.
[29] L. Ben Mansour, S. Chalbi and I. Ksentini, Experimental study of hydrodynamic and bubble size distributions in electroflotation process, Indian J. Chem. Technol., 14 (2007) 253–257.
[30] P. Painmanakul, Analyse locale du transfert de matière associé à la formation de bulles générées par différents types d'orifices dans différentes phases liquides Newtoniennes : étude expérimentale et modélisation, Doctoral thésis, INSA Toulouse, France, 2005.